



## Results from the Blazar Monitoring Campaign at the Whipple 10m Gamma-ray Telescope

DAVID STEELE<sup>1</sup>, FOR THE VERITAS COLLABORATION<sup>2</sup>

<sup>1</sup>*Adler Planetarium & Astronomy Museum, 1300 S. Lakeshore Dr., Chicago, IL 60605, USA*

<sup>2</sup>*For full author list see G. Maier, "VERITAS: Status and Latest Results", these proceedings*  
*dstele@adlerplanetarium.org*

**Abstract:** In September 2005, the observing program of the Whipple 10 m gamma-ray telescope was redefined to be dedicated almost exclusively to AGN monitoring. Since then the five Northern Hemisphere blazars that had already been detected at Whipple are monitored routinely each night that they are visible. Thanks to the efforts of a large number of multiwavelength collaborators, the first year of this program has been very successful. We report here on the analysis of Markarian 421 observations taken from November, 2005 to May, 2006 in the gamma-ray, X-ray, optical and radio bands.

### Introduction

Among active galactic nuclei (AGN), blazars are the most extreme and powerful sources known and are believed to have their jets more aligned with the line of sight than any other class of radio-loud AGN. Blazars are visible across the entire electromagnetic spectrum having a broad continuum extending from the radio through TeV  $\gamma$ -rays. They are high-luminosity objects, characterized by large, rapid, irregular amplitude variability in all accessible spectral bands. Their high level of variability makes long-term, well-sampled, multiwavelength (MWL) observations of blazars very important for constraining and understanding their emission mechanisms and characteristic time-scales.

Imaging atmospheric Cherenkov Telescopes (IACTs) are the only class of Very-High-Energy (VHE)  $\gamma$ -ray telescopes sensitive enough to monitor the short-term variability of blazars. However, IACT duty cycles are low ( $\sim 10\%$ ) because they can only operate on clear, moonless nights. In September 2005, the observing program of the Whipple 10 m Telescope was redefined to be dedicated almost exclusively to nightly blazar monitoring. Since that time the five Northern Hemisphere blazars that had already been detected at Whipple (Mrk 421, H1426+428, Mrk 501,

1ES 1959+650 and 1ES 2344+514) have been monitored routinely each night that they are visible above an elevation of  $60^\circ$ . For the first time, this has provided the opportunity to obtain long-term and well-sampled VHE light curves of these highly variable objects. Part of the motivation for these observations was to provide a trigger for more sensitive VHE observations of these AGN by the new generation of IACT telescopes (CANGAROO-III, HESS, MAGIC and VERITAS) and to provide baseline observations for similar observations with GLAST.

Here we will focus on the results of the monitoring campaign on Mrk 421. At a redshift of  $z=0.031$ , Mrk 421 was the first extragalactic source of VHE  $\gamma$ -rays to be discovered with ground-based telescopes [9]. Since then Mrk 421 has been studied extensively in the VHE regime and many periods of intense variability have been observed [3, 8, 1]. Mrk 421 is a high-frequency-peaked BL Lac (HBL) object exhibiting a non-thermal, broadband spectral energy distribution (SED) with two peaks, one in X-rays and a second in the TeV regime. The spectrum has been successfully reproduced by models where the X-ray peak is due to electron synchrotron radiation, and the TeV emission arises as the same electron population cools by inverse-Compton up-scattering of either the synchrotron photons (Synchrotron Self-Compton; SSC) or am-

bient photons (External Compton; EC) [7]. Like all such objects studied to date, the two peaks in the SED have been found to correlate with each other both in peak frequency and in strength.

The call for full multiwavelength coverage in previous campaigns was only invoked when large flares were observed in the TeV band. For the campaign reported in this work, we make no “a priori” assumptions about flux levels so that we can look for correlations on longer times scales and under different source conditions. Through the efforts of a large number of collaborators, a significant amount of data over the entire spectrum has been gathered on Mrk 421 during the 2005-2006 campaign. In this report we present light curves of radio, optical, X-ray and  $\gamma$ -ray data. We also show the results of a search for correlated emission between spectral bands and discuss the results in the context of SSC and EC models.

## Methods

All the TeV  $\gamma$ -ray observations presented here were made with the 10m Telescope at the Fred Lawrence Whipple Observatory (FLWO). During the period November 29, 2005 to May 29, 2006 a total of 98.0 hours of data were taken on Mrk 421. The data presented here were mostly taken in the *Tracking* mode since we were primarily interested in relative flux levels. The data were analyzed using the imaging technique and analysis procedures pioneered and developed by the Whipple Collaboration [4]. Since  $\gamma$ -ray air-shower images are known to be compact and elliptical in shape, while those generated by cosmic rays tend to be broader with more fluctuations, cuts were derived which reject approximately 99.7% of the background images while retaining over 50% of those generated by  $\gamma$ -ray showers. A large sample of dark-field data ( $\approx 200$  hours) spanning a similar zenith angle range was analyzed to estimate the background during AGN data runs. Although sensitive in the energy range from 200 GeV to 10 TeV, the peak response energy of the telescope to a Crab-like spectrum during the observations reported upon here was approximately 400 GeV (subject to a 20% uncertainty).

The X-ray data for this campaign were taken by the Rossi X-ray Timing Explorer (RXTE). Data from two of its three instruments, the Proportional Counter Array (PCA) and the All Sky Monitor (ASM) were used, but only the PCA data are presented here. The sensitive energy range of PCA is 3 - 15 keV, limited at the low-energy end by systematic effects in the detector, and at the high-energy end by low source counts above the background [6]. Mrk 421 was observed with the RXTE PCA from January 6 to May 31, 2006 in short daily exposures of 19 minutes, on average. Due to various observing constraints, the the X-ray and  $\gamma$ -ray observations were not always simultaneous, with the PCA observations starting on average 99 minutes behind the Whipple observations. Analysis of the PCA observations followed the standard procedure outlined in the RXTE Cookbook.

Eight optical observatories contributed data sets resulting in excellent optical coverage over almost the entire length of the campaign. They are the FLWO 1.2 m telescope; the Tenagra 0.8 m telescope in Tenagra, Arizona, USA; the Bradford Robotic Telescope in Tenerife, Canary Islands, Spain; the WIYN 0.9 m telescope at Kitt Peak, Arizona, USA; the 0.7 m telescope at Abastumani Observatory in Abastumani, Georgia; the 0.6 m Bell Observatory at Western Kentucky University, Bowling Green, Kentucky, USA; Bordeaux Observatory in Floirac, France; and the 1.05 m REOSC telescope at Osservatorio Astronomico di Torino, Italy.

The data from the various observatories were reduced and the photometry performed independently by different analysts using different strategies. Most analysts used relative aperture photometry performed using standard routines in IRAF [10]. Magnitudes were calculated with respect to one or more standard stars of Villata [11]. Because different observatories use different photometric systems, and photometric apertures and the definition of the reported measurement errors for each nightly-averaged flux are inconsistent across datasets, we have adopted a simple approach for the construction of the composite light curves whereby a unique flux offset is found for each spectral band of every instrument based on nearly simultaneous observations between participating observatories.

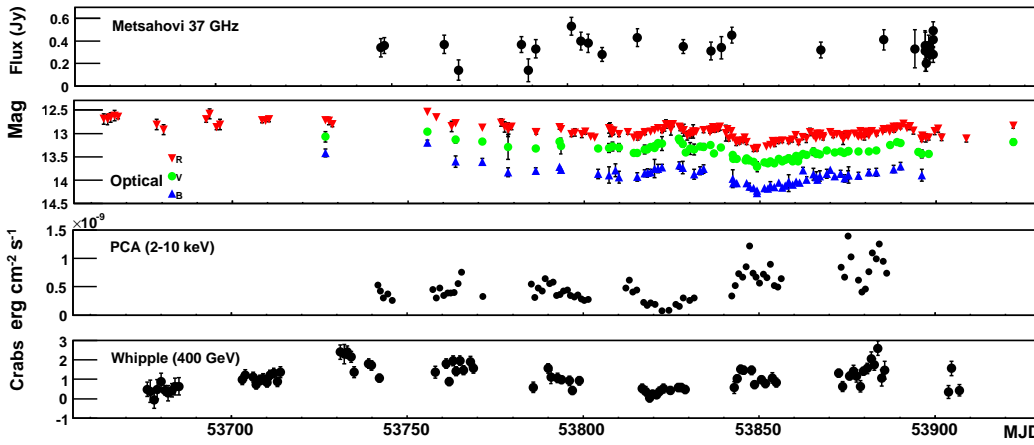


Figure 1: Radio, optical, X-ray and  $\gamma$ -ray light curves of Mrk 421 in 2005-2006.

The radio observations of this campaign come from three observatories taken at 10 frequencies: Metsähovi Radio Observatory, Kylmala, Finland (37 GHz), the University of Michigan Radio Astronomy Observatory, Dexter, Michigan, USA (4.8, 8.0 & 14.5 GHz), and the Radio Astronomical Telescope of the Academy of Sciences (RATAN-600), Zelenchuksky, Russia (1, 2.3, 4.8, 8, 11 & 22 GHz). Only the 37 GHz observations are reported here; the full set of radio data, (as well as a full X-ray and  $\gamma$ -ray spectral variability analysis) will be presented elsewhere. The observations from Metsähovi at 37 GHz have a bandwidth of 1 GHz and were obtained using the 14 m-diameter radio telescope.

The resulting light curves for the spectral bands described above are presented in Fig. 1. The source exhibits significant variability in all wavebands, with the level of variability generally higher in the energy regimes corresponding to the two peaks of the SED.

## Results & Discussion

Of all the pairs of light curves investigated, the X-ray and TeV light curves demonstrate the strongest correlation, as demonstrated by plotting the TeV flux vs. X-ray flux as in Fig. 2. The correlation suggests that the particle populations responsible for at least part of the emission in the two energy regimes are collocated, as is the case in the SSC scenario.

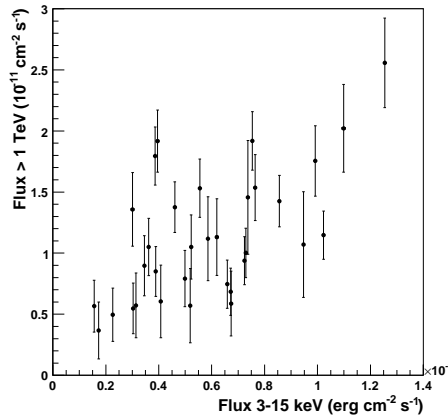


Figure 2: TeV  $\gamma$ -ray flux vs. X-ray flux (3-15 keV).

We searched for correlations between fluxes in other wavebands using the Discrete Correlation Function (DCF) [2]. The DCF gives the linear correlation coefficient ( $R$ ) for two light curves as a function of the time lag ( $\tau$ ) between them, and is well-suited to sparsely-sampled light curves. Besides the X-ray and TeV light curves, only the DCF between the optical and TeV light curves, presented in Fig. 3, warrants further investigation. The DCF indicates a possible correlation with the optical flux lagging the TeV flux by about 7 days. An elevated level of correlation is also seen with the optical leading the TeV by 25 to 60 days.

We investigated the significance of these possible correlations using simulated optical light curves with the same variability properties as the observed

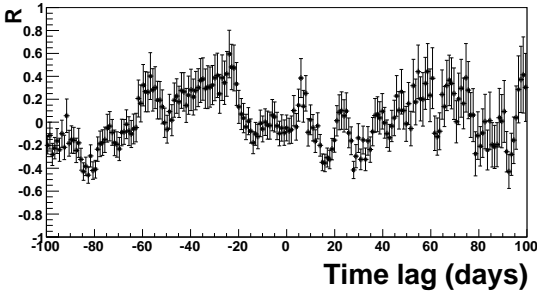


Figure 3: Discrete Correlation Function between the optical R-band and TeV band light curves. Positive values of time lag correspond to the optical flux lagging the TeV flux.

R-band light curve based on a Power Spectral Density (PSD) derived from a fit to the first-order structure function (SF). Assuming the process(es) responsible for the optical variability are stationary over the period of observation, the slope of the PSD,  $\beta$ , at a given variability frequency is related to the slope of the SF,  $\alpha$ , by  $\beta = 1 + \alpha$  [5].

After multiple realizations of the campaign using simulated, uncorrelated optical light curves we assess the probability to have seen the observed correlation features due to chance. For each bin of each simulated DCF, we record the values of the correlation coefficient,  $R$ , its error,  $\sigma_R$ , and  $S = R/\sigma_R$ . After many realizations, we build the distribution of  $S$  seen in each bin of the DCF and compute the chance probability,  $p_i$ , to have found  $S > S_{obs}$ . To assess the likelihood of the observed DCF features as a whole, we construct two more distributions,  $\mathcal{L}_{\pm} = \prod_i p_i$  where for  $\mathcal{L}_{-}$  ( $\mathcal{L}_{+}$ ) the product runs over all DCF bins with  $60 \text{ d} < \tau < 0$  ( $0 \leq \tau < 60 \text{ d}$ ). From these, we find the likelihood to have observed the optical precursor (optically-lagged) features by chance to be 20% (60%). Further investigation reveals that the lagged optical emission feature seen at  $\tau = 7 \text{ d}$  is likely due to contamination from the R-band auto-correlation function, which also exhibits alternate peaks and valleys at multiples of 7 days. The possible reality of the optical precursor emission is more difficult to interpret since our method assesses all the correlation features on a given side of the DCF at once. Unfortunately, it would not have been possible to assess a particular feature “a posteriori” without an unknown trials penalty.

## Conclusions

We have presented multiwavelength observations of the blazar Mrk421 taken during the first year of dedicated AGN monitoring with the Whipple 10 m Telescope. The TeV  $\gamma$ -ray and X-ray fluxes were well-correlated, consistent with previous observations of objects of this class. There was a weak indication that the optical flux may have led the TeV flux by 25 to 60 days, but a simulation reveals similar or stronger correlations arise by chance in one out of five simulated campaigns. If an optical precursor were observed conclusively, it could probe possible EC contributions to the TeV flux. We anticipate future long-term, multiwavelength observations will be important for further elucidation of AGN emission mechanisms.

## Acknowledgments

This research is supported by grants from the U.S. Department of Energy, the U.S. National Science Foundation, and the Smithsonian Institution, by NSERC in Canada, by PPARC in the UK and by Science Foundation Ireland. This research uses data from the High Energy Astrophysics Science Archive Research Center (HEASARC), provided by NASA’s Goddard Space Flight Center.

## References

- [1] M. Błażejowski et al. *ApJ*, 630:130, 2005.
- [2] R. A. Edelson and J. H. Krolik. *ApJ*, 333:646, 1988.
- [3] J. A. Gaidos et al. *Nature*, 383:319, 1996.
- [4] D. Horan. In *American Astron. Soc. Meeting Abstracts*, volume 209, page 109, 2007.
- [5] P. A. Hughes, H. D. Aller, and M. F. Aller. *ApJ*, 396:469, 1992.
- [6] K. Jahoda et al. In *Proc. SPIE VII*, volume 2808, page 59, 1996.
- [7] H. Krawczynski. *New Astron. Rev.*, 48:367, 2004.
- [8] D. Mazin et al. In *29th ICRC*, volume 4, page 327, 2005.
- [9] M. Punch et al. *Nature*, 358:477, 1992.
- [10] D. Tody. In *Proc. of Instrumentation in Astronomy VI; Part 2*, volume 627 of *SPIE*, page 733, 1986.
- [11] Villata et al. *A&AS*, 130:305, 1998.